

Single-Molecule Bonds Characterized by Solid-State Nanopore Force Spectroscopy

Vincent Tabard-Cossa,^{†,§} Matthew Wiggin,^{†,*} Dhruvi Trivedi,[†] Nahid N. Jetha,[†] Jason R. Dwyer,[†] and Andre Marziali^{†,*}

[†]Department of Physics and Astronomy and [‡]Department of Biochemistry & Molecular Biology, University of British Columbia, B.C., Canada. [§]Present address: Stanford Genome Technology Center, Stanford University, CA.

Noncovalent molecular bond energies are in the range of several $k_B T$, such that thermal activation plays a strong role in their strength and lifetime.¹ Application of force to a bond tilts the energy landscape along the force coordinate, lowering the energy barrier height and increasing the probability of dissociation. By measuring bond lifetime as the force is varied, bond rupture energies and lengths, and in some cases entire energy landscapes, can be reconstructed.^{1,2} Over the past two decades, a number of single-molecule techniques have emerged which measure rupture–force distributions or force–lifetime relationships of bonds, thereby providing details and mechanisms of molecular interactions.³ The ability to determine the strength of bonds between probe and target molecules makes force spectroscopy (FS) attractive as a highly specific molecular detection assay. Single-molecule force spectroscopy provides greater specificity in molecule recognition by reporting not only binding but also details of the bond between probe and analyte, thus discriminating against signal from nonspecific interactions. However, the cost, throughput, and complexity of optical traps, magnetic tweezers, and atomic force microscopes (AFM) have limited their use primarily to research applications.

Recently, we and others have established the utility of nanopore-based force spectroscopy (NFS) using α -hemolysin pores.^{4–7} However, the fragility of the supporting lipid membrane limits the range of forces that can be applied, and the lack of control over the pore geometry restricts the range of molecules that can be tested. Here, we present a robust, versatile solid-state NFS implementation and use it to directly

ABSTRACT Weak molecular interactions drive processes at the core of living systems, such as enzyme–substrate interactions, receptor–ligand binding, and nucleic acid replication. Single-molecule force spectroscopy is a remarkable tool for revealing molecular scale energy landscapes of noncovalent bonds, by exerting a mechanical force directly on an individual molecular complex and tracking its survival as a function of time and applied force. In principle, force spectroscopy methods can also be used for highly specific molecular recognition assays, by directly characterizing the strength of bonds between probe and target molecules. However, complexity and low throughput of conventional force spectroscopy techniques render such biosensing applications impractical. Here we demonstrate a straightforward single-molecule approach, suitable for both biophysical studies and molecular recognition assays, in which a ~ 3 nm silicon nitride nanopore is used to determine the bond lifetime spectrum of the biotin–neutravidin complex. Thousands of individual molecular complexes are captured and dissociated in the solid-state nanopore under constant applied forces, ranging from 400 to 900 mV, allowing us to extract the location of the energy barrier that governs the interaction, mapped at $\Delta x \approx 0.5$ nm. These results highlight the capacity of a solid-state nanopore to detect and characterize intermolecular interactions and demonstrate how this could be applied to rapid, highly specific molecular detection assays.

KEYWORDS: nanopore · force spectroscopy · molecular interactions · avidin–biotin · biosensors · biophysics

measure the strength of bonds between biological receptor molecules and their ligands.

The operation and instrumentation of NFS are greatly simplified compared to existing single-molecule technologies. Bond strengths of molecular complexes are studied without the need for elaborate chemistries to attach molecules to surfaces. The bonds can be formed in free solution long before the application of force, thus increasing the likelihood that the deepest energy minimum is reached before the pulling force is applied.²⁶ In addition, intricate single-molecule manipulation steps are eliminated since molecular complexes simply diffuse to the nanopore. Reporting is entirely electrical, obviating the need for complex and/or expensive optical components,

*Address correspondence to andre@physics.ubc.ca.

Received for review June 30, 2009 and accepted August 26, 2009.

Published online September 14, 2009.
10.1021/nn900713a CCC: \$40.75

© 2009 American Chemical Society

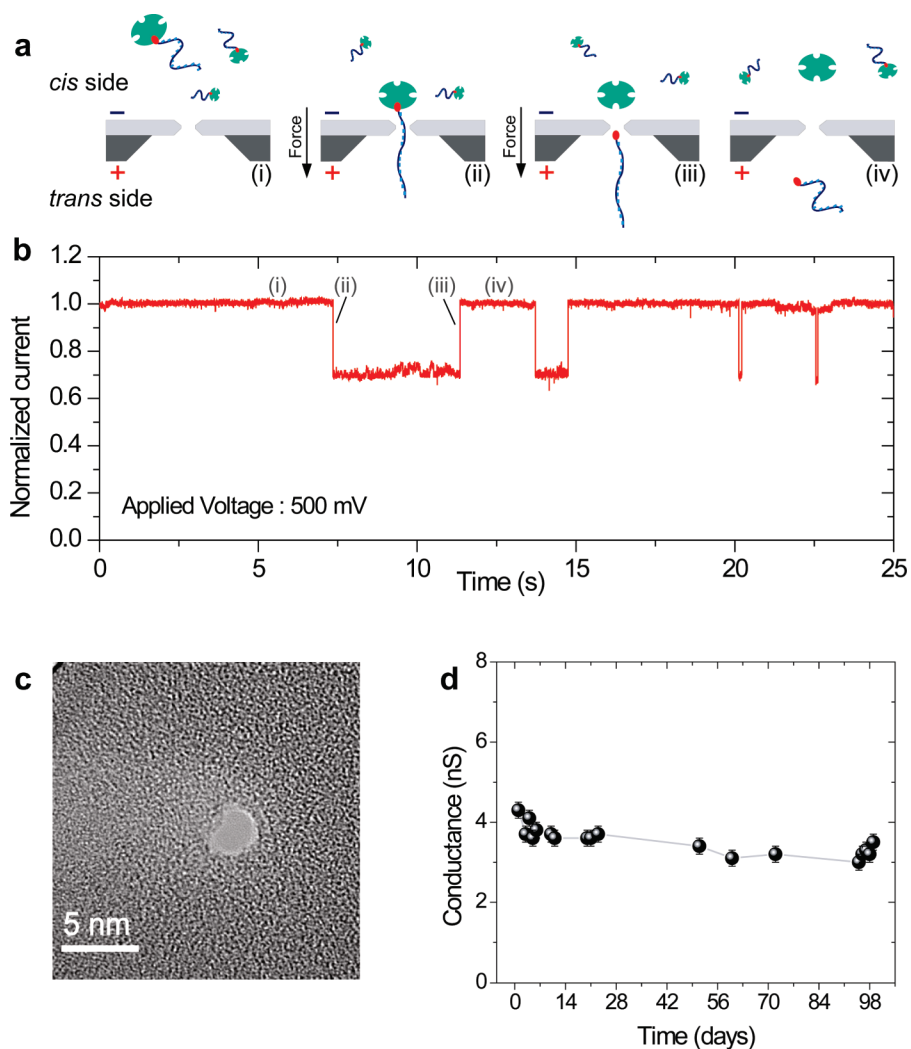


Figure 1. (a) Schematic of the nanopore force spectroscopy scheme used to measure the characteristic dissociation time scale for the neutravidin–biotin complex under constant pulling force. (i) Open pore, (ii) a biotinylated ssDNA molecule coupled to neutravidin is electrophoretically inserted into the pore. The size of the neutravidin protein prevents full translocation of the molecular complex. (iii) Electric field inside the pore pulls on the charged ssDNA, eventually breaking the receptor–ligand bond. (iv) Biotinylated ssDNA molecule translocates through to the *trans* side, while the neutravidin diffuses away from the pore on the *cis* side. (b) Ionic current trace showing four consecutive receptor–ligand dissociation events of varying duration. Experiments performed at room temperature, at +500 mV applied voltage, in 1 M KCl 10 mM HEPES buffered at pH 7.0. Current filtered at 1 kHz and sampled at 20 kHz. The ionic current is normalized to the average, open channel value. (c) Transmission electron microscope (TEM) image of the ~ 3 nm silicon nitride nanopore used for these experiments. (d) Nanopore conductance as a function of time. The high stability of the nanopore electrical characteristics enabled multiple force spectroscopy measurements to be repeated over an extended period of time to ascertain the reproducibility of the data.

requiring only two electrodes to control the transmembrane potential and measure changes in ionic current across the pore. These advantages make NFS well-suited for a wide range of applications, including molecular detection assays.

The method employs a nanometer-scale hole in an insulating membrane (*i.e.*, a nanopore) separating two reservoirs of electrolyte across which an electric potential is applied. The resulting ionic current flowing through the pore reports on the state of the pore as open or blocked. In contrast to other FS

methods, quantization of ionic current through the pore along with steric hindrance to pore entry easily selects for single-molecule events. The electric field inside the pore, ranging from 10^4 to 10^8 V/m, is used to apply force to charged molecules that are electrophoretically inserted into the nanopore. When the captured molecule is a nucleic acid oligomer, the forces applied are similar to most common FS techniques³ and can range from 0.1 to 10^3 pN. Various schemes can be designed to accommodate probing of different types of bonds, such as DNA–DNA interactions for genotyping applications, DNA–protein binding strengths for gene regulation studies, or receptor–ligand interactions for drug screening.

RESULTS AND DISCUSSION

To probe the strength of an individual neutravidin–biotin bond,^{9–13} biotin was covalently linked to a 94 nucleotide (nt) single-stranded DNA (ssDNA) molecule which serves to provide the electrostatic force on the bond. The bond between neutravidin and the biotinylated ssDNA is formed in free solution well before the application of force (see Methods). Individual neutravidin–biotin–ssDNA complexes are electrophoretically inserted from the *cis* side of a ~ 3 nm diameter silicon nitride nanopore (see Methods). The size of the neutravidin protein, *ca.* 5 nm in diameter,¹⁴ prevents full translocation of the

complex so that only the ssDNA molecule threads through the pore. The electric field within the pore pulls on the charged ssDNA, applying a force to the biotin–neutravidin bond. Under constant pulling force, the receptor–ligand pair eventually dissociates and the biotinylated ssDNA molecule rapidly translocates to the *trans* side of the nanopore while the uncharged neutravidin diffuses away on the *cis* side (as depicted in Figure 1a). We detect the capture of individual complexes under force as a reduction in ionic current and the return of the current to the open

channel state as a bond dissociation (see Figure 1b and Supporting Information). We note that captured molecules could also conceivably escape from the pore against the applied electric field, that is, back out toward the *cis* side, and that current traces for such events would appear similar to molecular complex dissociation events. However, under the experimental conditions, escape events are extremely rare and are not likely to be observed at all, as described in the Supporting Information.

Bond rupture in our experiments is thermally activated and therefore stochastic; we thus use the characteristic time scale for the bond lifetime, rather than an individual dissociation time, to characterize the process. For every applied force (voltage), many single-molecule events were timed and the corresponding cumulative distribution of dissociation times was calculated (Figure 2). This is the survival probability of the bond as a function of time ($P_{\text{survival}}(t)$), that is, the likelihood that biotin is still bound to neutravidin at time t after the ssDNA molecule is inserted into the pore. Measurements were made at voltages ranging between +400 and +900 mV. We refer the reader to the Supporting Information for histograms of ionic current levels for each applied potential. As expected, the dissociation time scale decreases with increasing force. To confirm that event times were governed by neutravidin–biotin dissociation, biotinylated ssDNA molecules lacking neutravidin were driven through the pore at similar voltages, resulting in events many orders of magnitude shorter than those ensuing from the complete complex (see Supporting Information).

The survival probability distributions plotted in Figure 2 do not decay exponentially with time. Similar non-exponential kinetics has also been observed in DNA duplex dissociation.^{4,5,15} We have recently demonstrated that subtle energetic perturbations ($\sim 2-5 k_B T$) can have a profound impact on the kinetics of DNA motion through nanopores. This behavior is attributed to variable DNA–pore interactions with the effect of stochastically altering the energy barrier height from one dissociation event to the next.¹⁶ Consequently, to extract characteristic dissociation time constants for the neutravidin–biotin complex, we fit the survival probability distributions to stretched exponential functions, of the form

$$P_{\text{survival}}(t) = A \exp[-(t/\tau_0)^\alpha] \quad (1)$$

where $0 < \alpha \leq 1$, and τ_0 (s) is a parameter with dimension of time. The term A accounts for a systematic error in detecting short events, due to detector bandwidth limitations (4-pole Bessel filter set to 1 kHz). This simple, yet versatile, decay function has been used to describe phenomena ranging from luminescence decay of fluorophores¹⁷ to single-molecule experiments of

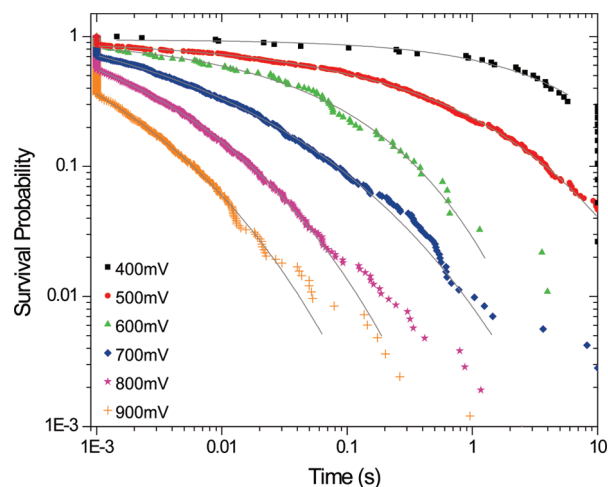


Figure 2. Cumulative distribution of dissociation times (*i.e.*, survival probability) for biotin bound to neutravidin. The survival probability for an applied force of +400 mV (black squares, 38 single-molecule events), +500 mV (red circles, 387 single-molecule events), +600 mV (green triangles, 92 single-molecule events), +700 mV (blue diamonds, 711 single-molecule events), +800 mV (magenta stars, 1049 single-molecule events), and +900 mV (orange crosses, 830 single-molecule events) are shown. Events lasting longer than 10 s are terminated by reversing the potential and are not timed but are counted in the total number of events for calculation of the survival probability. Similarly, events shorter than 1 ms are counted but not timed. Solid gray lines represent stretched exponential fits to the data from 0.001 to 10 s. Characteristic time scales from all fits obey Kramers' rule²⁵ as the voltage is varied.

DNA dissociation kinetics^{5,15} and protein conformational dynamics.¹⁸ Table 1 lists the values of the parameters used in each fit. Following Berberan–Santos *et al.*,¹⁷ we derive the expectation value of the time scale distribution from a stretched exponential survival probability distribution, given by

$$\langle \tau \rangle = \tau_0 \Gamma\left(1 + \frac{1}{\alpha}\right) \quad (2)$$

where Γ is the gamma function. This represents the characteristic bond lifetime, which is related to the dissociation energy barrier height by the Arrhenius relationship.

We use this characteristic time constant to analyze the relationship between dissociation time scale and

TABLE 1. Values of the Parameters Obtained from Stretched Exponential Fits

applied voltage (V)	τ_0 (s)	α	A^a	no. of events	R^2	$\langle \tau \rangle$ (s)
0.4	6.03	0.57	0.95	38	0.9791	9.72
0.5	0.39	0.36	0.95	387	0.9990	1.87
0.6	0.051	0.42	0.98	92	0.9939	0.145
0.7	9.1×10^{-4}	0.24	1.99	711	0.9992	0.0261
0.8	2.9×10^{-4}	0.28	2.30	1049	0.9996	0.00372
0.9	5×10^{-5}	0.26	3.17	830	0.9991	0.000930

^aThe rise in A above 600 mV is a direct result of the lack of time resolution below 1 ms due to the detector bandwidth limitation.

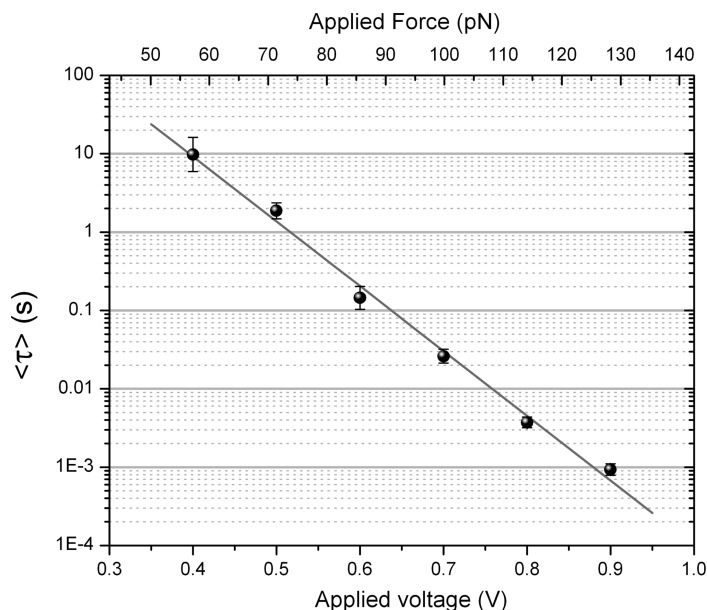


Figure 3. Characteristic dissociation time scale for neutravidin–biotin complexes as a function of the pulling force acting on the DNA strand. The force scale in Newton (top x-axis) is calculated for a nucleotide spacing of 0.45 nm and an effective charge of 0.4e. The solid line is an exponential fit to the data. Error bars indicate standard error of measurement, estimated using a bootstrap algorithm.

applied potential. Following Bell's postulate¹⁹ later adapted by Evans,²⁰ we employ a model inspired by Kramers' theory to describe the dynamics of the thermal dissociation of the receptor–ligand pair under constant applied force:

$$\langle \tau \rangle = \tau_D \exp \left[\frac{E_b}{k_B T} - \frac{f(V) \Delta x}{k_B T} \right] \quad (3)$$

where τ_D (s) is a diffusive relaxation time, E_b is the height of the energy barrier in the absence of applied force; Δx (m) is the width of the energy barrier measured in terms of separation of the ligand and receptor from their equilibrium value. Beyond the separation distance Δx , the intermolecular attractive forces become less than the applied force and the reaction becomes favorable. For a given energy barrier height, E_b , a longer energy barrier width, Δx , will decrease the gradient of energy along the direction of separation and thus reduce the bond strength; $f(V)$ (N) is the applied force, directly related to the applied voltage by

$$f(V) = z \cdot e \cdot \frac{n}{L} \cdot V \quad (4)$$

where $z \cdot e$ (C) is the effective charge of DNA inside the pore (see Supporting Information), V (V) the applied voltage, n the number of nucleotides in the pore, L (m) the length of the pore such that n/L is the inverse of the nucleotide spacing, that is $(0.45 \text{ nm})^{-1}$.

Figure 3 shows data confirming the exponential relationship between dissociation time scale and applied potential. The results reveal the large lifetime

spectrum expected for a bond sustained by weak noncovalent interactions. By pulling on the biotin–neutravidin bond at constant applied voltage, we directly probe the force-dependent lifetime of the molecular complex. Our results are complementary, but not directly comparable, to previous studies,¹³ which measured rupture–force distributions by ramping the force at constant pulling speed. Using eq 4, we can convert the applied potential to force,²¹ based on our previous estimate of the effective charge per nucleotide of 0.4e.¹⁶ We can then extract from Figure 3 the location of the prominent energy barrier that governs the strength of the biotin–neutravidin bond. The slope of the solid line in the biotin–neutravidin bond lifetime spectrum, defined as $\Delta x/k_B T$, infers the presence of an activation barrier at $\Delta x \approx 0.5 \text{ nm}$ along the direction of force. The accuracy of Δx will depend on the value of the effective charge of DNA used and, to a lesser degree, the direction of the force with respect to the molecular reaction coordinate. However, we note that this value is in agreement with previously reported results on streptavidin and avidin,^{8,11} for which the binding pockets are known to be chemically and structurally very similar.²²

CONCLUSIONS

This work demonstrates the potential of solid-state nanopore force spectroscopy as a technique to characterize the strength of bonds between biological receptor molecules and their ligands. A similar method may be used to study various molecular interaction systems, either taking advantage of the native target sizes or attaching the targets to appropriately sized particles and tagging the probe to a force-producing DNA polymer. We note that these results were acquired over an extended period of time (*ca.* 14 weeks) on a single nanopore, highlighting the fact that solid-state nanopores can be sufficiently robust for device integration and commercial deployment.

Under the stable experimental conditions achieved here, sufficient single-molecule events to characterize neutravidin–biotin interactions can be acquired in a few hours. Moreover, as demonstrated in previous work with organic pores,⁵ these measurements can be carried out in synchrony on arrays of nanopores, yielding the same information as repeated single-molecule measurements in a fraction of the time—typically minutes—and with no added complexity to the instrumentation. This approach can enable a high throughput, completely electronic method for detection and identification of biomolecules, with higher stringency than a simple hybridization or binding assay.

METHODS

Nanopore Fabrication. We fabricate pores with single-nanometer precision by exposing a $50 \times 50 \mu\text{m}$, 30 nm thick free-standing silicon nitride (SiN_x) membrane supported on a Si chip (TEM window grid by SPI) to a tightly focused high energy electron beam²³ (FEI Tecnai G2 operated at 200 kV TEM). Prolonged irradiation (ca. 30 s) of the SiN_x membrane with an electron beam focused to a spot of a few nanometers leads to the formation of a hole *via* sputtering.

Protocols and Instrumentation. Prior to mounting the nanopore chips in solution, the chips are submitted to a stringent cleaning procedure to render the surface hydrophilic and facilitate wetting of the pore, ensuring a low 1/f noise level.²⁴ The nanopore chips are immersed in a 3:1 mixture of concentrated sulfuric acid and hydrogen peroxide (piranha solution) and kept at 95 °C for 30 min. The chips are then thoroughly rinsed in filtered, degassed deionized water and immediately mounted in the liquid cell containing filtered, degassed 1 M KCl 10 mM HEPES buffered at pH 7.0. Nanopores mounted using this protocol present stable conductance for months.

A polytetrafluoroethylene cell was fabricated to mount the nanopore chip between two liquid reservoirs. Custom-made Viton gaskets sandwich the chip to ensure a GigaOhm seal as described in ref 24. Ag/AgCl electrodes immersed on both sides of the pore are connected to a patch clamp amplifier (Axopatch 200B, Axon Instruments) to measure changes in ionic current with picoamp sensitivity. The cell is placed in a Faraday enclosure to reduce electrical noise.

Data Acquisition and Analysis. Data acquisition and measurement automation were performed using custom-designed LabVIEW software controlling a National Instruments PCIe-6251 DAQ card to trigger the applied voltage on predetermined current levels. Data were low pass filtered at 1 kHz using the Axopatch 200B 4-pole Bessel filter and sampled at 20 kHz. Data analysis was carried out using custom-designed LabVIEW software to measure the duration of each current blockade, as described in the Results and Discussion.

Sample Preparation. 5'-Biotinylated oligonucleotides (94 nt 5'-poly(A)₃₀-C-poly(A)₂₉-C-poly(A)₁₉-CCACCAACCAACCC-3'), purified by ion exchange high pressure liquid chromatography, were purchased from Integrated DNA Technologies. Neutravidin proteins were purchased from Pierce (Thermo Fisher Scientific Inc.). Neutravidin, a deglycosylated variant of avidin, was chosen over avidin and streptavidin due to its particular isoelectric point (pI) of -6.3 ± 0.3 , which minimizes interactions with the electric field inside the pore under our experimental conditions (pH 7.0). Biotinylated oligonucleotides were mixed with neutravidin proteins in a 1:1 ratio at 10 μM concentration in 1 M KCl 10 mM HEPES pH7.0. Coupling between the two molecules was carried out at room temperature for 1 h before storing the working solution at -20 °C. An aliquot of the working solution is removed from the freezer on the day of each experiment. Sample concentrations of 20 or 100 nM were used for the different experiments.

Acknowledgment. The authors are grateful to D. Deamer, D. Stein, and B. Smith for fruitful discussions. We thank the past and present members of the UBC Applied Biophysics Laboratory, in particular, D. Broemeling, J. Nakane, and C. Tropini. We thank D. Branton for help with the instrument design; L. Yang for technical help on the TEM. This work was supported by the NIH (R01HG003248) and NSERC. V.T.-C. and M.W. acknowledge the financial support given by FQRNT (Postdoctoral Fellowship) and NSERC (Postgraduate Scholarship), respectively.

Supporting Information Available: Additional experimental details, ionic current histograms of single-molecule events, control experiments, discussion of escape kinetics, discussion of DNA/protein-pore interactions, extracted dissociation constant, and discussion of the effective charge of DNA inside a SiN_x nanopore. This material is available free of charge *via* the Internet at <http://pubs.acs.org>.

REFERENCES AND NOTES

- Evans, E. Probing the Relation between Force-Lifetime and Chemistry in Single Molecular Bonds. *Annu. Rev. Biophys. Biomol. Struct.* **2001**, *30*, 105–128.
- Dudko, O. K.; Hummer, G.; Szabo, A. Theory, Analysis, and Interpretation of Single-Molecule Force Spectroscopy Experiments. *Proc. Natl. Acad. Sci. U.S.A.* **2008**, *105*, 15755–15760.
- Neuman, K. C.; Nagy, A. Single-Molecule Force Spectroscopy: Optical Tweezers, Magnetic Tweezers and Atomic Force Microscopy. *Nat. Methods* **2008**, *5*, 491–505.
- Nakane, J.; Wiggin, M.; Marziali, A. A. Nanosensor for Transmembrane Capture and Identification of Single Nucleic Acid Molecules. *Biophys. J.* **2004**, *87*, 615–621.
- Tropini, C.; Marziali, A. Multi-Nanopore Force Spectroscopy for DNA Analysis. *Biophys. J.* **2007**, *92*, 1632–1637.
- Mathe, J.; Visram, H.; Viasnoff, V.; Rabin, Y.; Meller, A. Nanopore Unzipping of Individual DNA Hairpin Molecules. *Biophys. J.* **2004**, *87*, 3205–3212.
- Hornblower, B.; Coombs, A.; Whitaker, R. D.; Kolomeisky, A.; Picone, S. J.; Meller, A.; Akeson, M. Single-Molecule Analysis of DNA-Protein Complexes Using Nanopores. *Nat. Methods* **2007**, *4*, 315–317.
- Pincet, F.; Husson, J. The Solution to the Streptavidin-Biotin Paradox: The Influence of History on the Strength of Single Molecular Bonds. *Biophys. J.* **2005**, *89*, 4374–4381.
- Green, N. M.; Anfinsen, C. B.; Frederic, J. J. T. E.; Avidin, M. R. *Advances in Protein Chemistry*; Academic Press: New York, 1975; Vol. 29, pp 85–133.
- Lee, G. U.; Kidwell, D. A.; Colton, R. J. Sensing Discrete Streptavidin-Biotin Interactions with Atomic Force Microscopy. *Langmuir* **1994**, *10*, 354–357.
- Merkel, R.; Nassoy, P.; Leung, A.; Ritchie, K.; Evans, E. Energy Landscapes of Receptor-Ligand Bonds Explored with Dynamic Force Spectroscopy. *Nature* **1999**, *397*, 50–53.
- Grubmüller, H.; Heymann, B.; Tavan, P. Ligand Binding: Molecular Mechanics Calculation of the Streptavidin-Biotin Rupture Force. *Science* **1996**, *271*, 997–999.
- Walton, E. B.; Lee, S.; Van Vliet, K. J. Extending Bell's Model: How Force Transducer Stiffness Alters Measured Unbinding Forces and Kinetics of Molecular Complexes. *Biophys. J.* **2008**, *94*, 2621–2630.
- Vermette, P.; Gengenbach, T.; Divisekera, U.; Kambouris, P. A.; Griesser, H. J.; Meagher, L. Immobilization and Surface Characterization of NeutrAvidin Biotin-Binding Protein on Different Hydrogel Interlayers. *J. Colloid Interface Sci.* **2003**, *259*, 13–26.
- Biancanello, P. L.; Kim, A. J.; Crocker, J. C. Long-Time Stretched Exponential Kinetics in Single DNA Duplex Dissociation. *Biophys. J.* **2008**, *94*, 891–896.
- Wiggin, M.; Tropini, C.; Tabard-Cossa, V.; Jetha, N. N.; Marziali, A. Nonexponential Kinetics of DNA Escape from α -Hemolysin Nanopores. *Biophys. J.* **2008**, *95*, 5317–5323.
- Berberan-Santos, M. N.; Bodunov, E. N.; Valeur, B. Mathematical Functions for the Analysis of Luminescence Decays with Underlying Distributions 1. Kohlrausch Decay Function (Stretched Exponential). *Chem. Phys.* **2005**, *315*, 171–182.
- Yang, H.; Luo, G.; Karnchanaphanurach, P.; Louie, T.-M.; Rech, I.; Cova, S.; Xun, L.; Xie, X. S. Protein Conformational Dynamics Probed by Single-Molecule Electron Transfer. *Science* **2003**, *302*, 262–266.
- Bell, G. Models for the Specific Adhesion of Cells to Cells. *Science* **1978**, *200*, 618–627.
- Evans, E.; Ritchie, K. Dynamic Strength of Molecular Adhesion Bonds. *Biophys. J.* **1997**, *72*, 1541–1555.
- Keyser, U. F.; Koeleman, B. N.; Van Dorp, S.; Krapf, D.; Smeets, R. M. M.; Lemay, S. G.; Dekker, N. H.; Dekker, C. Direct Force Measurements on DNA in a Solid-State Nanopore. *Nat. Phys.* **2006**, *2*, 473–477.

22. Hiller, Y.; Gershoni, J. M.; Bayer, E. A.; Wilchek, M. Biotin Binding to Avidin. Oligosaccharide Side Chain Not Required for Ligand Association. *Biochem. J.* **1987**, *248*, 167–171.
23. Wu, M.-Y.; Krapf, D.; Zandbergen, M.; Zandbergen, H.; Batson, P. E. Formation of Nanopores in a SiN/SiO₂ Membrane with an Electron Beam. *Appl. Phys. Lett.* **2005**, *87*, 113106-3.
24. Tabard-Cossa, V.; Trivedi, D.; Wiggin, M.; Jetha, N. N.; Marziali, A. Noise Analysis and Reduction in Solid-State Nanopores. *Nanotechnology* **2007**, *18*, 305505.
25. Hanggi, P.; Talkner, P.; Borkovec, M. Reaction-Rate Theory—50 Years after Kramers. *Rev. Mod. Phys.* **1990**, *62*, 251–341.
26. In other FS methods, the bonds are often formed when two functionalized surfaces are brought into contact for very short times (milliseconds to seconds), thus potentially not allowing the system enough time to reach its most stable state and introducing effects from the history of its formation.⁸